Astron. Astrophys. 341, 587–594 (1999)

ASTRONOMY AND ASTROPHYSICS

Thermal balance of electrons in calculations of model stellar atmospheres

Jiří Kubát[1], **Joachim Puls**[2], **and Adalbert W.A. Pauldrach**[2]

[1] Astronomický ústav, Akademie věd České republiky, CZ-251 65 Ondřejov, Czech Republic
[2] Institut für Astronomie und Astrophysik, Scheinerstrasse 1, D-81679 München, Germany

Received 17 July 1998 / Accepted 23 October 1998

Abstract. As an alternative to the equation of radiative equilibrium, the equation of thermal balance of electrons is used in order to derive temperature structures in NLTE model stellar atmospheres. The calculations are accomplished for various stellar parameters comprising different stellar types, and both methods are compared. It turns out that the application of the electron thermal balance equation is superior to using the standard equation of radiative equilibrium in the outer, line forming parts of stellar atmospheres and beyond.

Key words: radiation mechanisms: thermal – methods: numerical – stars: atmospheres

1. Introduction

The numerical modeling of a NLTE stellar atmosphere is a complex task. In order to determine the atmospheric structure it is necessary to solve for all variables throughout the atmosphere, i.e., temperature, electron density, population numbers, radial distance, velocity fields, etc. All quantities have to be calculated globally and simultaneously. Thus, it is natural to seek for methods that enable to lower the computational costs necessary both for the model calculation and for the solution of a particular equation. The determination of the temperature structure (in parallel with all other variables) of a stellar atmosphere is the most time consuming part of such a calculation.

The complicated interaction between radiation and atomic population numbers causes drastic changes of temperature, especially in the outer atmospheric layers. Although the computational time per iteration is almost the same as if the temperature were fixed (i.e., all variables except temperature are solved), the number of iterations necessary to obtain a converged solution is considerably larger when the temperature is solved for as well. The computer codes that are aiming at such a correct temperature determination usually need a huge amount of computational time to find a consistent NLTE solution, and they quickly become hardly usable for a *routine* analysis of a larger number of stars.

There are two commonly used ways of calculating temperatures in the determination of NLTE model atmospheres. The first one uses the condition of constant flux (flux correction, or the differential form of radiative equilibrium), the second one is based on the integral form of the condition of radiative equilibrium. The flux correction method is useful at large optical depths, since it ensures flux conservation. Its application to NLTE model atmospheres calculations was described, e.g., by Gustafsson (1971), Frandsen (1974), Hubeny (1988) and Kubát (1996).

The condition of radiative equilibrium is commonly used for determining the temperature stratification throughout the line forming regions and also in the optically thin part of the atmosphere. First NLTE calculations of model atmospheres that considered the equation of radiative equilibrium were performed by Feautrier (1968) and by Auer & Mihalas (1969a). Subsequently, Auer & Mihalas (1969b) incorporated the equation of radiative equilibrium into their method of complete linearization. It became standard for a variety of computer codes (e.g., Mihalas et al. 1975, Kudritzki 1976, Hubeny 1975, 1988 for the plane parallel static case; Mihalas & Hummer 1974, Gruschinske 1978 for the spherically symmetric static case). The new generation of codes based on the accelerated lambda iteration method (Werner 1986, Gabler et al. 1989, Hamann & Wessolowski 1990) also determines the temperature structure using the equation of radiative equilibrium.

The NLTE blanketing codes (e.g., Schmutz 1991, Dreizler & Werner 1993, Hubeny & Lanz 1995) solving for the temperature structure require an enormous amount of computational time (depending on the number of elements included and the numerical efficiency of the code), and are consequently well suited only for the analysis of individual stars or smaller subsets. For a *routine* analysis of larger stellar samples, however, they are of only limited practical use (see also Pauldrach et al. 1997, Hillier & Miller 1998). In order to tackle the latter problem, Santolaya-Rey et al. (1997) decided to develop an extremely fast NLTE model atmosphere/line formation code. This was enabled by several substantial approximations regarding temperature and density structure. The most severe restriction was the assumption of a constant temperature in the outer parts of the atmosphere.

Keeping in mind the basic strategy of Santolaya-Rey et al., we made several attempts to find faster methods for the determination of the temperature structure than the one by using the

Send offprint requests to: J. Kubát

equation of radiative equilibrium. Here we report on first results of applying the method of thermal balance of electrons.

2. Energy equilibrium in stellar atmospheres

Let us assume that energy is transported through the stellar atmosphere only via radiation, i.e., we neglect convection. Therefore, we restrict our analysis to hot stars, where atmospheric convection is not so important.

2.1. Radiative equilibrium

The condition of radiative equilibrium (see, e.g., Unsöld, 1955, or Mihalas 1978)

$$4\pi \int_0^\infty (\kappa_\nu J_\nu - \eta_\nu)\,\mathrm{d}\nu = 0 \tag{1}$$

became a standard equation for temperature determinations in the outer atmospheric layers ($\tau_R \lesssim 2/3$) in the course of constructing model stellar atmospheres both in LTE and NLTE. For a discussion of various methods to calculate LTE radiative equilibrium model atmospheres, see Mihalas (1978). Here we shall consider only the NLTE case.

In Eq. (1), κ_ν is the total opacity, η_ν the total emissivity, and J_ν the mean intensity of the radiation field. This expression accounts only for the radiative energy balance and simply states that the total amount of radiative energy absorbed at a particular depth ($4\pi\int_0^\infty \kappa_\nu J_\nu \mathrm{d}\nu$) equals the total amount of emitted radiative energy ($4\pi\int_0^\infty \eta_\nu \mathrm{d}\nu$). The exchange of energy takes place with the internal energy of atoms (via bound-bound and bound-free transitions) and with the kinetic energy of electrons (via bound-free and free-free transitions).

Thus we have three dominant energy pools (radiation, internal atomic energy, and kinetic energy of electrons – temperature).

In standard calculations of NLTE model atmospheres, the equation of radiative equilibrium is being solved in parallel with the equations of statistical equilibrium, radiative transfer and the equation of motion, which for static atmospheres reduces to the equation of hydrostatic equilibrium.

Within this standard framework, however, our experience shows that for some particular stellar parameters it is either almost impossible to obtain convergence towards the correct solution or that the convergence rate is rather slow. This indicates that the condition of radiative equilibrium may not be the best formulation for certain combinations of basic stellar parameters.

The reason for the fault is simple. With respect to the transitions included into the equation of radiative equilibrium, only bound-free and free-free processes *directly* affect the temperature, whereas bound-bound radiative transitions have an only indirect effect via the equations of statistical equilibrium.

Thus, if the bound-bound transitions dominate the radiative energy balance, the real important transitions are numerically “killed” and the result is a slow convergence of temperature.

2.2. Thermal balance of electrons

As an alternative to the equation of radiative equilibrium, it is possible to use the equation for the thermal balance of electrons. This equation considers heating and cooling of an electron gas by collisions with atoms, by radiative ionization and recombination, and direct radiation heating and cooling via free-free transitions.

This approach, of course, is not new. Since the pioneering work by Hummer & Seaton (1963) and Hummer (1963), it has been widely used for the study of planetary nebulae (e.g. Williams 1967, Ferland & Truran 1981, see also Osterbrock 1974 and Aller 1984). Nevertheless, its application to models of stellar atmospheres remains isolated. Some of the few examples are the calculations by Drew (1985, 1989), who used this method to determine wind temperatures of OB stars, and more recently by Pauldrach et al. (1997) and Hillier & Miller (1998). The equation for the thermal balance of electrons follows from the Boltzmann kinetic equation, and for equilibrium we have (e.g., Lifshitz & Pitaevski 1979)

$$Q^{\mathrm{H}} - Q^{\mathrm{C}} = 0, \tag{2}$$

where Q^{H} is the total amount of energy supplied to electrons (heating) and Q^{C} corresponds to the inverse process (cooling). Let us consider the physical mechanisms which control the thermal balance of electrons and radiative equilibrium in detail.

2.3. Free-free transitions

Free-free transitions transfer energy between the radiation field and electrons. The total amount of energy transferred from radiation to electrons via absorption (heating) can be expressed as

$$Q^{\mathrm{H}}_{\mathrm{ff}} = 4\pi n_e \sum_j N_j \int_0^\infty \alpha_{\mathrm{ff},j}(\nu,T) J_\nu \mathrm{d}\nu \tag{3}$$

where n_e is the electron density, N_j the NLTE population of the ion j, $\alpha_{\mathrm{ff},j}(\nu,T)$ is the free-free absorption cross section, T stands for temperature, and J_ν is the mean intensity of radiation. Similarly, for the inverse process (cooling), the total amount of transferred energy is

$$\begin{aligned} Q^{\mathrm{C}}_{\mathrm{ff}} \;=\; & 4\pi n_e \sum_j N_j \int_0^\infty \alpha_{\mathrm{ff},j}(\nu,T) \left(J_\nu + \frac{2h\nu^3}{c^2}\right) \times \\ & \times e^{-h\nu/kT} \mathrm{d}\nu. \end{aligned} \tag{4}$$

where h is the Planck constant, k is the Boltzmann constant, and c is the speed of light. The free-free heating and cooling terms also enter the equation of radiative equilibrium. Thus, free-free radiative losses are $R^{\mathrm{L}}_{\mathrm{ff}} = Q^{\mathrm{H}}_{\mathrm{ff}}$ and free-free radiative gains $R^{\mathrm{G}}_{\mathrm{ff}} = Q^{\mathrm{C}}_{\mathrm{ff}}$.

2.4. Bound-free transitions

Bound-free transitions transfer energy between the radiation field and both electrons and atoms. Since we are dealing with the thermal balance of *electrons*, we shall consider only the energy transferred to electrons (and back), so that the part of the energy transferred to atoms must be subtracted. The corresponding expression for heating by ionization reads

$$Q_{\rm bf}^{\rm H} = 4\pi \sum_{l,k} n_l^* b_l w_k \int_0^\infty \alpha_{{\rm bf},\,lk}(\nu) J_\nu \left(1 - \frac{\nu_{lk}}{\nu}\right) {\rm d}\nu. \qquad (5)$$

Here n_l^* is the LTE population of the lower bound level, b_l is the corresponding departure coefficient, w_k is the occupation probability of the upper level (see Kubát 1997), ν_{lk} is the frequency of the ionization edge, and $\alpha_{{\rm bf},\,lk}(\nu)$ is the corresponding photoionization cross-section (note that below the ionization edge $\alpha_{{\rm bf},\,lk}(\nu) = 0$). Similarly, for cooling holds

$$Q_{\rm bf}^{\rm C} = 4\pi \sum_{l,k} n_l^* b_k w_l \int_0^\infty \alpha_{{\rm bf},\,lk}(\nu) \left(J_\nu + \frac{2h\nu^3}{c^2}\right) \times e^{-h\nu/kT} \left(1 - \frac{\nu_{lk}}{\nu}\right) {\rm d}\nu. \qquad (6)$$

In this equation, w_l is the occupation probability of the lower level. The atomic level occupation probabilities were introduced by Hummer & Mihalas (1988) to account for a more precise cutoff of the highest atomic levels than by standard methods. Their implementation to model atmosphere codes is described by Hubeny et al. (1994) and Kubát (1997). For high gravity stars (white dwarfs) with extreme dense lower atmospheres, they are important. For low gravity stars with corresponding lower densities, however, it is acceptable to set $w_l = 1$ for all explicit levels.

On the other hand, the standard expressions for bound-free radiative losses and gains are a bit different, since they concern the total radiative energy pool. The radiative losses are

$$R_{\rm bf}^{\rm L} = 4\pi \sum_{l,k} n_l^* b_l w_k \int_0^\infty \alpha_{{\rm bf},\,lk}(\nu) J_\nu {\rm d}\nu. \qquad (7)$$

and the radiative gains

$$R_{\rm bf}^{\rm G} = 4\pi \sum_{l,k} n_l^* b_k w_l \int_0^\infty \alpha_{{\rm bf},\,lk}(\nu) \left(J_\nu + \frac{2h\nu^3}{c^2}\right) \times e^{-h\nu/kT} {\rm d}\nu. \qquad (8)$$

2.5. Bound-bound transitions

Bound-bound transitions transfer energy between radiation and atoms. They concern only the radiative equilibrium, not the thermal one. The bound-bound radiative losses are

$$R_{\rm bb}^{\rm L} = 4\pi \sum_{l,m} n_l^* b_l w_m \int_0^\infty \alpha_{{\rm bb},\,lm}(\nu) J_\nu {\rm d}\nu. \qquad (9)$$

and the radiative gains

$$R_{\rm bb}^{\rm G} = 4\pi \sum_{l,m} n_m^* b_m w_l \int_0^\infty \alpha_{{\rm bb},\,lm}(\nu) \left(J_\nu + \frac{2h\nu^3}{c^2}\right) \times e^{-h\nu/kT} {\rm d}\nu. \qquad (10)$$

Here n_l^*, b_l, and w_l is the LTE population, departure coefficient, and occupation probability for the lower level l (and similarly for the upper level m), and $\alpha_{{\rm bb},\,lm}(\nu) = (\pi e^2/m_e c^2) f_{lm} \phi(\nu)$. In the last expression, e is the electron charge, m_e is the electron mass, c is the speed of light, f_{lm} is the oscillator strength, and $\phi(\nu)$ is the line profile.

2.6. Collisions

Collisions transfer energy between electrons and atoms, they do not affect the radiation field. For collisional deexcitation or recombination (heating) we use the expression with occupation probabilities w_m (see Kubát 1997)

$$Q_{\rm c}^{\rm H} = n_e \sum_{l,m} b_m n_l^* w_m q_{lm}(T) h\nu_{lm}. \qquad (11)$$

Here $q_{lm}(T)$ is the collision strength, l denotes the lower level, and m is the index of the upper level. For cooling collisional terms (excitation and ionization), the following equation is valid,

$$Q_{\rm c}^{\rm C} = n_e \sum_{l,m} b_l n_l^* w_m q_{lm}(T) h\nu_{lm}. \qquad (12)$$

Note, that $Q_{\rm c}^{\rm C} = Q_{\rm c}^{\rm H}$ holds in LTE, since $b_l = b_m = 1$.

2.7. Total radiative equilibrium and thermal balance equations

Combining Eqs. (3), (4), (7), (8), (9), and (10), we obtain the total radiative equilibrium equation (1). On the other hand, combining Eqs. (3), (4), (5), (6), (11), and (12), we obtain the total thermal balance equation (2).

3. Comparison of radiative equilibrium and thermal balance methods

In order to investigate in how far an application of the electron thermal balance is appropriate, we compared it with the standard equation of radiative equilibrium. To this end, we calculated very simple static spherically symmetric pure hydrogen and hydrogen-helium NLTE model atmospheres for several stellar parameters comprising different spectral types.

3.1. Model atoms

Our hydrogen model atom consists of ten levels of H I plus continuum. The atomic data (for hydrogen) are as follows: The oscillator strengths are after Wiese et al. (1966), lines were assumed to have depth independent Doppler profiles. The photoionization cross sections are calculated using the standard formula (e.g. Mihalas 1978, Eqs. 4-114). The free-free cross section is calculated by means of Eqs. 4-122 in Mihalas (1978). Gaunt factors both for bound-free and free-free transitions are evaluated using fits by Mihalas (1967). Collisional ionization rates are determined using the polynomial fit by Napiwotzki (1993). For calculation of collisional excitation rates, the expressions in Mihalas et al. (1975) were used.

Table 1. Summary of the atomic data used for model atmosphere calculation

	radiative			collisional	
ion	b-b	b-f	f-f	b-b	b-f
H I	1	2	3	5	4
He I	1	7	3	6	6
He II	1	2	3	6	4

Notes: 1 – Wiese et al. (1966); 2 – Mihalas (1978) Eqs. 4-114, Gaunt factors after Mihalas (1967); 3 – Mihalas (1978) Eqs. 4-122, Gaunt factors after Mihalas (1967); 4 – Napiwotzki (1993) polynomial fit; 5 – Mihalas et al. (1975); 6 – Mihalas & Stone (1968); 7 – Koester et al. (1985) for $n \leq 3$, hydrogenic (2) for higher n.

Our helium model atom consists of 29 levels of He I, 20 levels of He II plus He III. All levels of He I up to $n = 4$ are considered separately, levels with $5 \leq n \leq 9$ are joined into two levels for each n, one for singlets and the second one for triplets. The oscillator strengths are also after Wiese et al. (1966). The He I photoionization cross sections for $n \leq 3$ are calculated after Koester et al. (1985), for higher n they are assumed to be hydrogenic. The He II photoionization cross sections are taken as hydrogenic. The free-free cross section is calculated similar to the case of hydrogen. All collisional rates for He I and collisional excitation rates for He II are calculated after Mihalas & Stone (1968). Collisional ionization rates for He II are calculated using the polynomial fit by Napiwotzki (1993). This set of atomic data is summarized in Table 1.

3.2. Computer program

We used the computer code described by Kubát (1994, 1996, 1997) with the appropriate modifications allowing for the inclusion of electron thermal balance. It calculates temperature, density, radius and population numbers assuming hydrostatic, radiative and statistical equilibrium. These equations are solved using a linearization (Newton-Raphson) method, whereas the radiative transfer equation is solved by means of approximate lambda operators.

We calculated two sets of models, the first one using the equation of radiative equilibrium, whereas the latter was replaced by the equation of electron thermal balance in the second set. Although Newton-Raphson (linearization of temperature, electron density and departure coefficients in parallel) was used in both cases, test calculations showed that the much simpler approach of linearizing only the temperature terms works satisfactorily as well. Note, that we always applied the flux correction method to determine the temperature structure in the optically thick parts ($\tau_R \gtrsim 2/3$) of the atmosphere.

3.3. Results

The results presented in this section concentrate on the outer atmosphere ($\tau_R \lesssim 2/3$), since by using the flux correction method in the inner part we have successfully ensured the conservation of total flux.

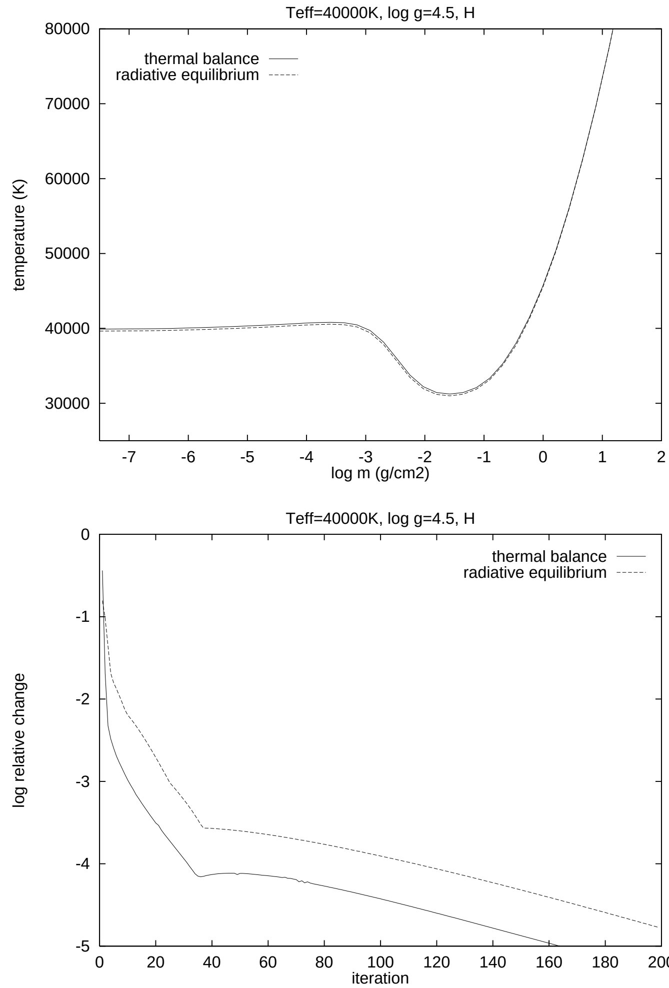

Fig. 1. Temperature structure (*upper panel*) and convergence of the temperature (*lower panel*) for the pure hydrogen NLTE model atmosphere with all lines considered for $T_{\text{eff}} = 40000\text{K}$, $\log g = 4.5$ and $R = 15R_{\odot}$.

3.3.1. O star model

For a spherically symmetric O star model, we choose the following basic parameters: luminosity $L = 5.2 \cdot 10^5 L_{\odot}$, radius $R = 15R_{\odot}$, and, in order to enable the static approximation, the rather unrealistic mass $M = 260M_{\odot}$. These parameters give $T_{\text{eff}} = 40000\text{K}$ and $\log g = 4.5$.

We started our calculation from a converged LTE model for the above parameters. The resulting temperature profiles are plotted in Fig. 1 (pure hydrogen model) and Fig. 2 (hydrogen-helium model). The method of using radiative equilibrium failed to converge for the case of the full hydrogen-helium model with all lines. Nevertheless, by putting the He II Lyman lines into detailed radiative balance, we could compare the convergence rate of both methods also for hydrogen-helium models. The difference between the models resulting from our alternative

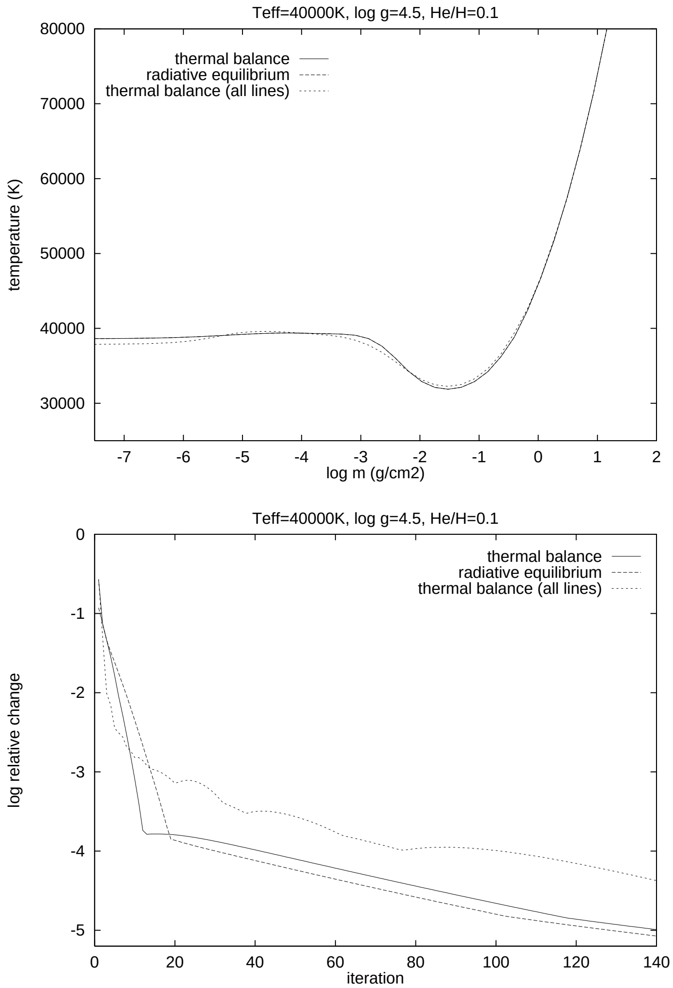

Fig. 2. Temperature structure (*upper panel*) and convergence of the temperature (*lower panel*) for the hydrogen-helium NLTE model atmosphere with all lines considered (dotted line) and He II Lyman lines set into detailed balance (fully drawn and dashed lines) for $T_{\rm eff} = 40000{\rm K}$, $\log g = 4.5$ and $R = 15R_{\odot}$. The ratio $N_{\rm He}/N_{\rm H} = 0.1$.

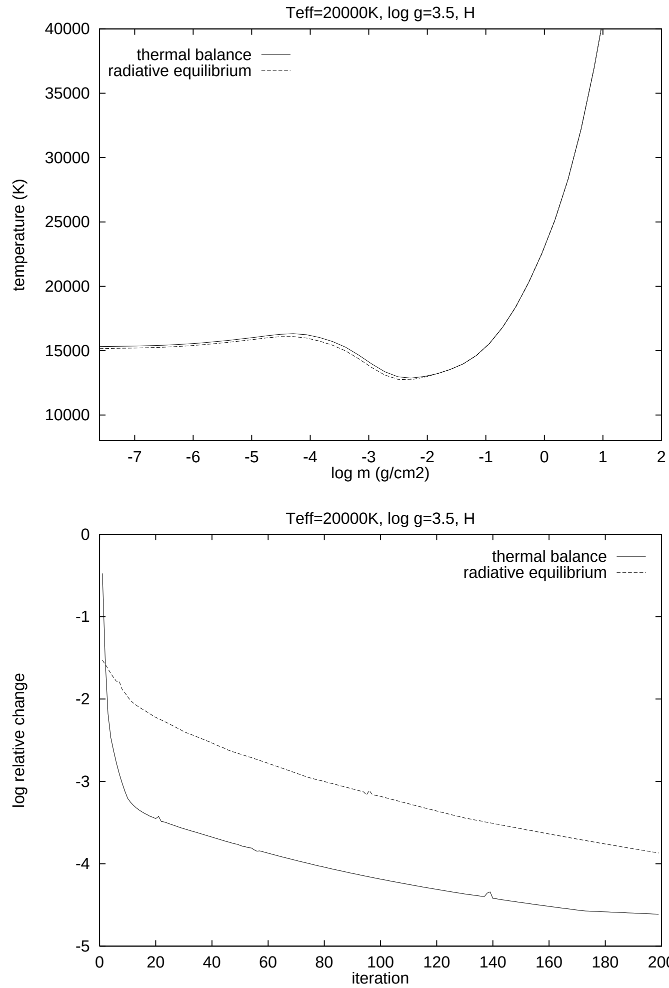

Fig. 3. Temperature structure (*upper panel*) and convergence of the temperature (*lower panel*) for the pure hydrogen NLTE model atmosphere with all lines except L_α considered (the L_α line is set to the detailed radiative balance) for $T_{\rm eff} = 20000{\rm K}$, $\log g = 3.5$ and $R = 10R_{\odot}$.

energy equations is negligible both for the pure hydrogen as well as the hydrogen-helium model.

The convergence rate for the pure hydrogen model is displayed in the lower panel of Fig. 1. Both methods converge well, although the convergence for the electron thermal balance equation is significantly better. Similar conclusions can be drawn for the hydrogen-helium models (lower panel of Fig. 2). Thus we may conclude that for the case of O stars the method of electron thermal balance is superior.

3.3.2. B star model

We have chosen the following parameters for a "typical" B star: luminosity $L = 1.44 \cdot 10^4 L_{\odot}$, radius $R = 10R_{\odot}$ and mass $M = 11.5M_{\odot}$, which yield $T_{\rm eff} = 20000{\rm K}$ and $\log g = 3.5$.

Similar to the O-star case, we started our calculation from a converged LTE model for the above parameters, and we have calculated both pure hydrogen and hydrogen-helium models. For both models, the hydrogen Lyman-α line was set into the detailed radiative balance. In addition, the hydrogen-helium models were calculated using the assumption of detailed balance in He II Lyman lines. They are optically thick throughout the atmosphere, and, in addition, their influence on the temperature structure is negligible due to the weak radiation field at their transition frequencies. The resulting temperature profiles are displayed in Figs. 3 and 4. The difference between both of them is very small. The convergence of temperature is displayed in the lower panel of Figs. 3 and 4.

In conclusion, for this B star parameter range the method of using the electron thermal balance is much better suited than the standard radiative equilibrium approach.

3.3.3. Hot white dwarfs models

As an example for a hot white dwarf, we have chosen a star with luminosity $L = 1.48 \cdot 10^3 L_{\odot}$, radius $R = 0.13R_{\odot}$ and mass

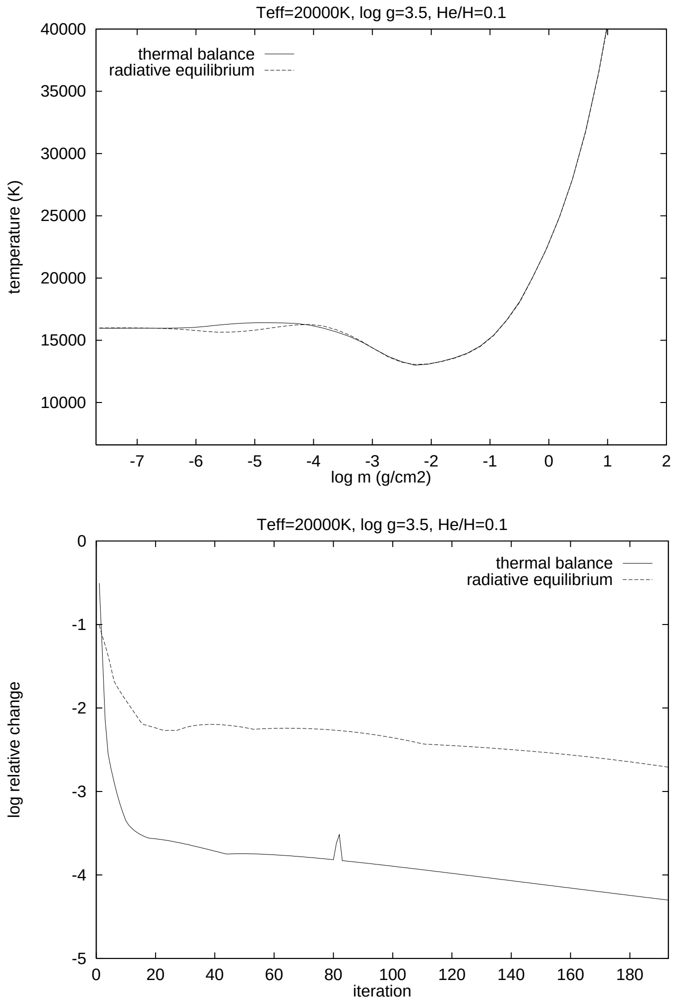

Fig. 4. Temperature structure (*upper panel*) and temperature convergence (*lower panel*) for the hydrogen-helium NLTE model atmosphere with all lines considered (except hydrogen Lyman-α line and He II Lyman lines set into detailed balance) for $T_{\rm eff} = 20000$K, $\log g = 3.5$ and $R = 10R_{\odot}$. The ratio $N_{\rm He}/N_{\rm H} = 0.1$.

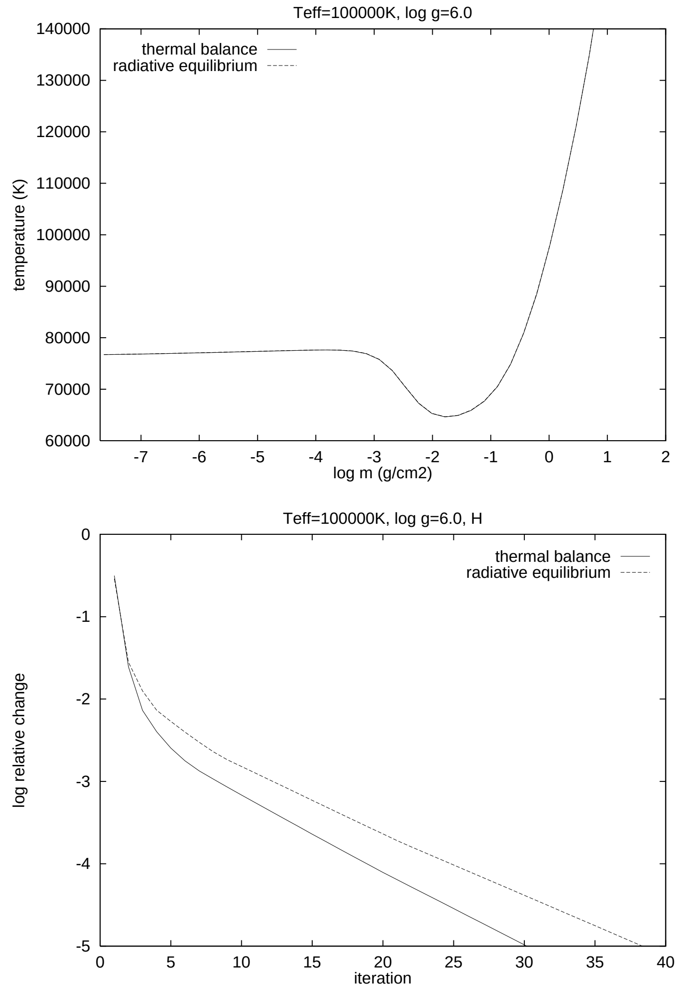

Fig. 5. The same as Fig. 1 for the hot white dwarf model with $T_{\rm eff} = 100000$K, $\log g = 6.0$ and $R = 0.13R_{\odot}$.

$M = 0.6M_{\odot}$ (a typical white dwarf mass), yielding $T_{\rm eff} = 100000$K and $\log g = 6.0$.

The hydrogen-helium models were calculated using the assumption of detailed balance in the He II Lyman lines. The results are displayed in Figs. 5 and 6. Contrary to the case of B stars, no differences are visible and the models are almost identical.

Both models converge quickly for both methods, so that for hot white dwarf models the use of radiative equilibrium remains acceptable. Note, however, that even here the electron thermal balance method converges faster.

3.3.4. Cooler white dwarfs models

A slightly different situation is encountered for the case of cooler white dwarfs. As a representative example, we have chosen a model with luminosity $L = 1.2L_{\odot}$, radius $R = 0.04R_{\odot}$, and again a typical white dwarf mass $M = 0.6M_{\odot}$. These parameters give $T_{\rm eff} = 30000$K and $\log g = 7.0$.

For this model then and for the *pure hydrogen* atmosphere, our findings are consistent with the above results for the hotter star, i.e. identical temperature structures and a better convergence of the electron thermal balance method (Fig. 7). A different situation applies for the hydrogen-helium model. Here, the use of radiative equilibrium resulted in divergence caused by He II Lyman continuum, whereas the electron thermal balance method converged relatively fast to a reasonable temperature structure (Fig. 8). The electron thermal balance method overcomes the instability caused by this transition and is consequently better suited also in this case.

4. Discussion

The results of the preceding section showed the supremacy of calculations based on the electron thermal balance, compared to the standard equation of radiative equilibrium, at least for our model parameters. The better performance is more striking in cases where strong optically thick lines exist in those

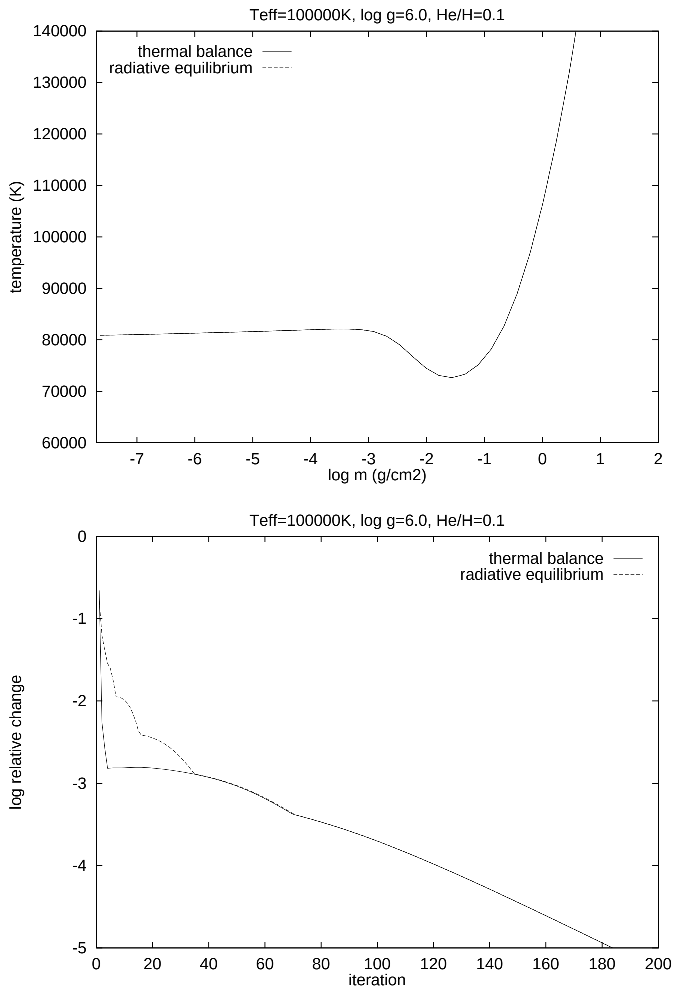

Fig. 6. Temperature structure (*upper panel*) and convergence of the temperature (*lower panel*) for the hydrogen-helium NLTE model atmosphere with all lines considered (except He II Lyman lines set into detailed balance) for $T_{\rm eff} = 100000{\rm K}$, $\log g = 6.0$ and $R = 0.13 R_{\odot}$. The ratio $Y_{\rm He}/Y_{\rm He} = 0.1$.

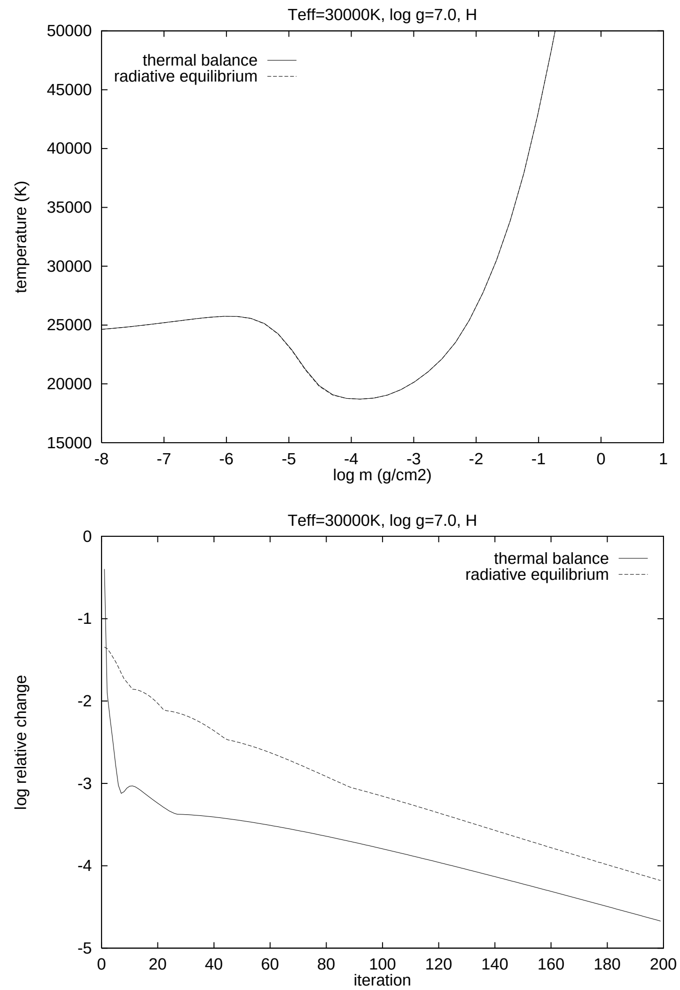

Fig. 7. The same as Fig. 1 for $T_{\rm eff} = 30000{\rm K}$, $\log g = 7.0$ and $R = 0.04 R_{\odot}$.

atmospheric regions where the continuum is optically thin. The basic difference between these two methods lies in the treatment of lines. It must be emphasized that line radiative rates do not explicitly depend on temperature.

For optically thin continua and optically thick lines most of the absorbed radiative energy is absorbed in line transitions. Only a minor part is absorbed (and re-emitted) in the continuum. Since the electron thermal balance equation does not consider radiative line processes at all, these strong lines do not directly affect the temperature. On the other hand, the equation of radiative equilibrium considers lines which may completely dominate the radiative equilibrium balance in the extreme cases of strong lines formation far outside the atmosphere. In consequence, radiative equilibrium is not able to extract the important information from the bound-free and free-free rates, which are numerically "killed" by unimportant information from bound-bound rates. (Note, however, that by a consistent use of the ALI-formalism also in the equation of radiative equilibrium,

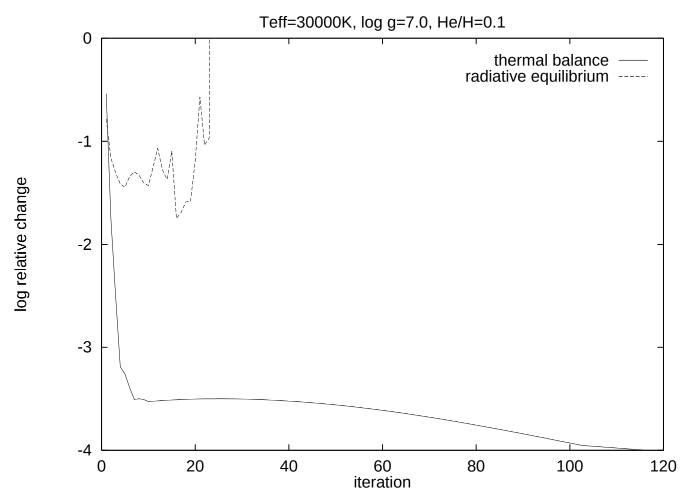

Fig. 8. Convergence of the temperature for the hydrogen-helium NLTE model atmosphere with all lines considered (except He II Lyman set into detailed balance) for $T_{\rm eff} = 30000{\rm K}$, $\log g = 7.0$ and $R = 0.04 R_{\odot}$. The ratio $N_{\rm He}/N_{\rm H} = 0.1$.

the “effective” bound-bound rates entering the energy balance can be largely reduced compared to their actual value.) Especially in the outer parts of the atmosphere, where a couple of strong lines are still optically thick when the continuum has already become optically thin, this dominance of bound-bound rates is a specific severe problem. On the other hand, our consideration also explains why radiative equilibrium works well for hot white dwarfs. These objects have no *extended* region where optically thick lines and an optically thin continuum exists in parallel, since the lines are formed just above the photosphere.

The new method of electron thermal balance has also the very desirable feature that the convergence is fastest over the first three decades of relative changes, which is the typical number where normal models are considered as being converged. In these first decades the comparison between the two methods extremely favors the new one.

We should also mention some difficulties of the electron thermal balance method. The electron thermal balance method occasionally fails just above the point where $\tau_{\rm R} = 2/3$, i.e., the point where we usually switch from flux correction (differential form) to the integral description of radiative equilibrium. This was true, e.g., for the cool white dwarf models described above. The easiest way to overcome this problem is to use radiative equilibrium for the (usually few) critical depth points and to switch to the electron thermal balance just above them. The fast convergence of the electron thermal balance method is preserved and the scheme is stable again. On the other hand, no failure of the electron thermal balance method was observed when the departure coefficients were kept fixed in the linearization step and recalculated later.

One might also argue that the supremacy of the electron thermal balance method may be due to some hidden fault in our linearization scheme for the radiative equilibrium method. This possibility can not be completely excluded, but it seems to be unprobable. The fact that the model atmospheres of the hottest stars converge quickly even by using the radiative equilibrium method lowers the possibility of such a fault. In any case, the method of thermal balance of electrons has proven its efficiency. Of course, it would be highly desirable if somebody repeats this comparison study using a completely independent code.

5. Conclusions

We have compared two methods of determining the temperature in the outer parts of stellar model atmospheres. The first one uses the equation of radiative equilibrium, the second one the equation of thermal balance of electrons. We have shown that the latter method yields a faster convergence rate and that it is able to overcome the difficulties caused by strong optically thick lines, where the method using radiative equilibrium fails. Therefore we highly recommend this method for calculating temperature stratifications in stellar atmosphere models.

Acknowledgements. We like to thank Dr. Ivan Hubeny for useful comments and suggestions to improve the paper. This research has made use of NASA’s Astrophysics Data System Abstract Service. J.K. would like to thank for the support and the hospitality of the Universitätssternwarte München. This work was supported by the Max Planck Institut für Astrophysik (Garching), by a grant of the Grant Agency of the Czech Republic (GA ČR) 205/96/1198, and by projects K1-003-601/4 and K1-043-601.

References

Aller L.H., 1984, Physics of Thermal Gaseous Nebulae. D. Reidel Publ. Comp., Dordrecht
Auer L.H., Mihalas D., 1969a, ApJ 156, 157
Auer L.H., Mihalas D., 1969b, ApJ 158, 641
Dreizler S., Werner K., 1993, A&A 278, 199
Drew J., 1985, MNRAS 217, 867
Drew J., 1989, ApJS 71, 267
Ferland G.J., Truran J.W., 1981, ApJ 244, 1022
Frandsen S., 1974, A&A 37, 139
Gabler R., Gabler A., Kudritzki R.P., Puls J., Pauldrach A., 1989, A&A 226, 162
Gruschinske J., 1978, Ph.D. Thesis, Universität Kiel
Gustafsson B., 1971, A&A 10, 187
Hamann W.-R., Wessolowski U., 1990, A&A 227, 171
Hillier D.J., Miller D.L., 1998, ApJ 496, 407
Hubený I., 1975, Bull. Astron. Inst. Czech. 26, 38
Hubeny I., 1988, Comput. Phys. Commun. 52, 103
Hubeny I., Lanz T., 1995, ApJ 439, 875
Hummer D.G., 1963, MNRAS 125, 461
Hummer D.G., Seaton M.J., 1963, MNRAS 125, 437
Koester D., Vauclair G., Dolez N., et al., 1985, A&A 149, 423
Kubát J., 1994, A&A 287, 179
Kubát J., 1996, A&A 305, 255
Kubát J., 1997, A&A 326, 277
Kudritzki R.P., 1976, A&A 52, 11
Lifshitz E.M., Pitaevski L.P., 1979, Fizicheskaya Kinetika, Nauka, Moskva
Mihalas D., 1967, ApJ 149, 169
Mihalas D., 1978, Stellar Atmospheres. 2nd ed., W.H.Freeman & Comp., San Francisco
Mihalas D., Hummer D.G., 1974, ApJS 28, 343
Mihalas D., Stone M.E., 1968, ApJ 151, 293
Mihalas D., Heasley J.N., Auer L.H., 1975, NCAR-TN/STR-104, NCAR Boulder
Napiwotzki R., 1993, Ph.D. thesis, Universität Kiel
Osterbrock D.E., 1974, Astrophysics of Gaseous Nebulae. W.H.Freeman & Comp., San Francisco
Pauldrach A.W.A., Lennon M., Hoffmann T.L., et al., 1997, In: Howarth I.D. (ed.) Properties of Hot, Luminous Stars. Boulder-Munich Workshop II, ASP Conf.Ser. Vol.131, p. 258
Santolaya-Rey A.E., Puls J., Herrero A., 1997, A&A 323, 488
Schmutz W., 1991, In: Crivellari L., Hubeny I., Hummer D.G. (eds.) Stellar Atmospheres: Beyond Classical Models. NATO ASI Series C, Vol. 141, p. 191
Unsöld A., 1955, Physik der Sternatmosphären. Springer Verlag Berlin
Werner K., 1986, A&A 161, 177
Wiese W.L., Smith M.W., Glennon B.M., 1966, Atomic Transition Probabilities. Vol.I., Hydrogen Through Neon. NSRDS-NBS 4 Washington D.C.
Williams R.E., 1967, ApJ 147, 556